The use of magnetic iron oxide based nanoparticles to improve microalgae harvesting in real wastewater

Ahmad Abo Markeb[1,2], Jordi Llimós-Turet[1], Ivet Ferrer[3], Paqui Blanquez[1], Amanda Alonso[1], Antoni Sánchez[1], Javier Moral-Vico[1,*], Xavier Font[1]

[1]Departament of Chemical, Biological and Environmental Engineering. Escola d'Enginyeria. Universitat Autònoma de Barcelona. 08193 Bellaterra (Spain).

[2]Departament of Chemistry. Faculty of Science. Assiut University. 71516-Assiut (Egypt).

[3]GEMMA – Group of Environmental Engineering and Microbiology, Department of Civil and Environmental Engineering, Universitat Politècnica de Catalunya-BarcelonaTech, c/Jordi Girona 1-3, Building D1, E-08034, Barcelona (Spain).

[*]Corresponding Author:

Javier Moral-Vico

Tel: 935812789

Email: AntonioJavier.Moral@uab.cat

Abstract

A novel approach for harvesting *Scenedesmus* sp. microalgae from real wastewater by using adsorbents of magnetite-based nanoparticles (Fe_3O_4 NPs) was tested in this study for the first time for this microalgae. Using these NPs, the harvesting efficiency was even higher than 95%. The optimal conditions (0.14 gNPs/L, a short magnetic separation time of only 8 min and 27 min of contact time) were found using the response surface methodology. The best fitting of the adsorption equilibrium results was achieved by the Langmuir isotherm model, and the maximum adsorption capacity for *Scenedesmus* sp. reached 3.49 g dry cell weight (DCW)/g Fe_3O_4 NPs. Zeta potential measurements and the Dubinin-Radushkevich isotherm model analysis pointed out that the main adsorption mechanism between *Scenedesmus* sp. cells and Fe_3O_4 NPs was electrostatic interaction. Finally, Fe_3O_4 NPs were six times successfully reused by combining an alkaline treatment with an ultrasonication process, which implies microalgae lysis. The results herein obtained highlight the potential for magnetic separation of microalgae from wastewater, which is capable of reaching a high harvesting efficiency in a very short time.

Keywords: Biomass recovery; Microalgal biomass; Wastewater; Magnetite nanoparticles; Response surface methodology

1. Introduction

Microalgae are nowadays cultured to produce high value-added compounds like nutraceuticals and pharmaceuticals (Jha et al., 2017). During the last decade, much attention has been paid to the production of non-food bioproducts like biofuels or biopolymers (Milano et al., 2016; Özçimen et al., 2017). Regarding biofuels, the main advantages of microalgae over terrestrial crops are: i) their high photosynthetic efficiency, which leads to a high growth rate and biomass production; ii) no competition with food crops for arable land and; iii) the accumulation of certain compounds (e.g. lipids or carbohydrates) under stress conditions (Khan et al., 2018). On the other hand, the main disadvantages are: i) the requirement of high amounts of water and nutrients and; ii) microalgal biomass harvesting (Valigore et al., 2012). The first barrier can be overcome by using wastewater, which already has a high concentration of nutrients and thus, must be treated (Arbib et al., 2014). Indeed, this alternative provides a public service along with a valuable biomass feedstock. High Rate Algal Ponds (HRAP) are typically used for secondary wastewater treatment, while open or closed photobioreactors maybe used for the tertiary treatment. However, microalgae harvesting is still a challenge.

When microalgae are harvested to produce high value-added compounds, the cost of biomass harvesting is not a barrier. Indeed, energy intensive processes as centrifugation, which achieves relatively high solids concentration (e.g. 10%) (Benemann, 2013; Singh et al., 2011) are generally used. However, in the context of biofuels or biopolymers, these processes are not affordable (Dassey et al., 2013). When wastewater is used to produce microalgae, the presence of bacteria in the culture enhances floc formation and eases biomass separation by gravity settling, which can reach a biomass recovery of 70-80% or even higher (90%) through biomass recycling (Gutiérrez et al., 2016). Gravity settling and dissolved air flotation could be further enhanced by coagulation-flocculation with

chemicals, with low energy requirements if compared to centrifugation. In this sense, natural products like starch and tannin–based flocculants have shown promising results (Gutiérrez et al., 2015a; Gutiérrez et al., 2015b). The main drawback is that the addition of chemicals has an economic cost and can affect downstream processing of harvested biomass. Besides, when pure microalgae cultures are used, gravity settling only achieves a biomass recovery of 50-60%. Although flocculation is the most commonly used microalgae harvesting method (Vandamme et al., 2013), subsequent sedimentation needs a long time and the harvesting efficiency is still low (Wang et al., 2014; Wang et al. 2016).

In the recent years, an increasing attention has been paid to microalgae harvesting by means of magnetophoretic separation, due to the time-saving and a simplified synthesis of nanoparticles and their reusability (Hu et al., 2013; Prochazkova et al., 2013a). Specifically, magnetic nanoparticles (NPs) have been investigated due to their high specific surface area, and biocompatibility, but also to the fact that they can adhere to microalgae cells and then be easily separated from the medium by applying an external magnetic field (Schwertmann et al., 2007; Procházková et al., 2012). Moreover, both the stability of the NPs suspension and the harvesting efficiency can be enhanced by surface coating or modification of magnetic nanoparticles with diverse materials such as polymers and surfactants (Wang et al., 2016; Ge et al., 2015; Lin et al., 2015). To date, different types of magnetic NPs (Fe_3O_4 NPs), with and without surface coating, have been tested to harvest microalgae such as the oleaginous *Chlorella* sp. (Wang et al., 2016), *Scenedesmus dimorphus* (Ge et al., 2015a) and *Chlorella vulgaris* (Prochazkova et al., 2013a). However, to authors' knowledge, this is the first study performed with these iron based nanomaterials for harvesting *Scenedesmus* sp. as microalgae model in a real wastewater.

Firstly, the harvesting efficiency of different synthesized NPs and the effect of NPs coating was screened. Secondly, the best synthesized NPs were used to optimize the microalgae

separation process in terms of harvesting efficiency, NPs contact time and magnetic separation time. Finally, the maximum adsorption capacity and reusability of synthesized NPs was evaluated.

2. Materials and Methods

2.1 Nanoparticles synthesis

2.1.1 *Materials*

Iron (II) chloride ($FeCl_2$), Iron (III) chloride hexahydrate ($FeCl_3.6H_2O$), polyethyleneimine (PEI), 3-Aminopropyl triethoxysilane ($SiO\text{-}NH_2$) (APTES), and cetyltrimethyl ammonium bromide (CTAB), were purchased from Sigma-Aldrich (Barcelona, Spain). Sodium hydroxide pellets (NaOH) were purchased from Merck (Spain). All the chemicals were of analytical grade or higher. All nanoparticles reported were fabricated in our laboratory.

2.1.2 *Magnetite (Fe_3O_4) NPs synthesis*

Fe_3O_4 NPs were prepared using the co-precipitation method slightly modified as reported previously (Abo Markeb et al., 2016). Briefly, two different concentrations of $FeCl_2$ and $FeCl_3 \cdot 6H_2O$, prepared by keeping the Fe^{2+}/Fe^{3+} molar ratio of 1:2 and coded as Fe_3O_4 NPs-I (25 and 50 mM) and Fe_3O_4 NPs-II (100 and 200 mM), were dissolved in 100 mL of deoxygenated ultrapure water (Milli-Q). Then, the suspension of each mixture of iron salts was incubated for 1 hour at 40°C under nitrogen atmosphere. After that, 0.5 M NaOH solution was added dropwise into each of the mixed solutions of the iron salt solution under agitation until a pH of 9.0 was achieved. During the titration process, the formation of Fe_3O_4 NPs was confirmed when the mixture's colour turned from light yellow to red-brown and then eventually to black. Then, the suspension containing Fe_3O_4 NPs was stirred continuously for 1 hour at 40°C and under nitrogen atmosphere. Afterwards, the NPs were

separated using a neodymium permanent magnet (NdFeB) and washed three times using ultrapure water, followed by a final ethanol washing and then dried at 60°C for 12 hours.

2.1.3 CTAB coated Fe_3O_4 NPs

Cetyltrimethylammonium bromide (CTAB) coated Fe_3O_4 NPs-II were prepared with a slight modification of the reported method (Khoshnevisan et al. 2012). The obtained black Fe_3O_4 NPs (section 2.3.1) were sonicated for 20 min in 100 mL of ultrapure water (Milli-Q), followed by the addition of CTAB dropwise to obtain a weight ratio of 1:1 between CTAB and Fe_3O_4 NPs-II. Then, the mixture was continuously stirred for 30 min at room temperature. Subsequently, Fe_3O_4@CTAB NPs were separated using aNdFeB permanent magnet and washed using ultrapure water, followed by ethanol washing and then dried at 60°C for 12 hours.

2.1.4 PEI-modified Fe_3O_4 NPs

Coating of Fe_3O_4 NPs-II with polyethyleneimine (PEI) was performed with slight modifications of the reported method (Ge et al. 2015). Briefly, 1 g of Fe_3O_4 NPs was dispersed in 100 mL ultrapure water (Milli-Q) by sonication for 20 min. Then, 2.5 g of PEI were titrated into Fe_3O_4 NPs suspension. After that, the mixture was continuously stirred for 30 min at room temperature. Later, Fe_3O_4@PEI NPs were washed with water and ethanol respectively, separated using NdFeB permanent magnet and dried at 60°C for 12 hours.

2.1.5 Amine functionalized Fe_3O_4 NPs

Production of the NPs containing amine groups by functionalization of Fe_3O_4 NPs-II with aminopropyltriethoxysilane (APTES) was carried out by a modification of the reported

147 method (Hasanzadeh et al., 2017; Yazid et al., 2017). Briefly, 1 g of Fe_3O_4 NPs was
148 dispersed in 100 mL ultra-pure (Milli-Q) water for 20 min. Then, 1 mL of APTES was
149 added dropwise to the suspension of NPs and the mixture was continuously stirred for 12
150 hours at room temperature. Later, magnetic NPs were washed three times using ultrapure
151 water, magnetically separated and finally dried overnight at 60°C.
152
153 ***2.2 Microalgae production***
154 Microalgae were produced in a pilot plant that treats real wastewater from the municipal
155 sewer system in Barcelona (Spain). In this plant, wastewater undergoes a screening
156 pretreatment, primary treatment in gravity settlers (7 L) and secondary treatment in high
157 rate algal ponds (HRAPs) (0.5 m^3, 1.5 m^2) followed by clarifiers (9 L) that separate
158 microalgal biomass from the treated effluent. This wastewater treatment system is located
159 outdoors, as previously reported (Gutiérrez et al. 2016). Harvested microalgal biomass is
160 thickened and digested in 3 lab-scale anaerobic reactors (1.5 L) with a hydraulic retention
161 time (HRT) of 20 days under mesophilic conditions, as described previously (Passos et al.
162 2015).The digestate is then diluted in secondary effluent from the clarifier (1:50 v:v) and
163 treated in an airlift-photobioreactor (30 L) located indoors. At the time the experiments
164 were conducted, the HRT was 10 days and light-dark cycles of 12h. Light was supplied by
165 an external lamp (600 W, Sunmaster, USA) placed at 80 cm from the photobioreactor,
166 providing 19,000 lux (289 μmol/m^2s) (Arias et al., 2018). Average biomass concentration
167 was 0.63 g TSS/L and 0.36 g VSS/L, the turbidity 327 NTU and pH 7.38. It consisted of a
168 mixed culture clearly dominated by *Scenedesmus* sp. (99.8%), that are, finally,
169 anaerobically digested (Arias et al., 2018).
170
171 ***2.3 Characterization of nanoparticles and microalgae***

2.3.1 Inductively coupled plasma optical emission spectrometry, ICP-OES

The metal content of NPs was analyzed by using ICP-OES (Perkin Elmer model Optima 4300DV). Pre-treatment of the samples consisted of an acid digestion, dilution, and filtration using 0.45 μm Nylon filters. The concentration of the metal was reported in terms of mg_{Fe}/g_{NPs} (where g_{NPs} refers to the total mass of the NPs). Analyses were externally performed at the *Servei d'Anàlisi Química*, Universitat Autònoma de Barcelona (UAB), Spain.

2.3.2 Scanning Electron Microscopy and Transmission Electron Microscopy

a) Nanoparticles characterization: the morphology and size of the NPs were characterized, on one hand, using a Zeiss Merlin Scanning Electron Microscopy (SEM) and, on the other hand, using a JEM-2011/JEOL, High-Resolution Transmission Electron Microscopy (HR-TEM) equipped with Energy-Dispersive Spectroscopy (EDS). Measurements were acquired with an Oxford INCA X-MAX detector at the *Servei de Microscopia* at UAB, Spain. 3 different TEM images were studied with ImageJ software to evaluate NPs average sizes.

b) Microalgae-NPs interaction: microalgae harvesting using the magnetite-based NPs was characterized both using a Zeiss Merlin Scanning Electron Microscopy (SEM) and using a JEM-2011/JEOL, High-Resolution Transmission Electron Microscopy (HR-TEM) equipped with Energy-Dispersive Spectroscopy (EDS). TEM was used for the cross-sectioned analysis of prepared samples as reported in a previous study (Zhang et al. 2016). Briefly, the pellets were firstly obtained by centrifugating the samples for 10 min at 3000 rpm. Next, cells were fixed with 2.5% glutaraldehyde in 0.1 M phosphate buffer (pH 7.0) at 4 °C overnight, rinsed twice with the phosphate buffer (pH 7.0), then post-fixed with 1% OsO_4 in a 0.1 M phosphate buffer (pH 7.0) at 4 °C for 4 h and again rinsed twice with the

197 phosphate buffer (pH 7.0). After fixation, dehydration of sample cells was performed by a
198 washing series of ethanol (50%, 70% and 90%), a 1:1 mixture of ethanol (90%) and
199 acetone (90%), followed by washing with acetone (90%) and finally acetone (100%) at
200 4°C for 15 min at each step. Following, samples were immersed in 1:1 and 1:2 mixtures of
201 acetone and ethoxyline resin for 1 h and 4 h, respectively, transferred to ethoxyline resin at
202 room temperature overnight, placed in a baking box and heated at 60°C for 48 h. Then, the
203 cross sections were obtained by embedding the ultra-thin sections of samples in epoxy
204 resin after cutting using a 35° diamond knife from Diatomeanda Leica UC7
205 ultramicrotome. Finally, the cross-sectioning part was stained with uranyl acetate and lead
206 citrate.
207
208 ***2.3.3*** *Microalgae analysis*
209 The microalgae culture was characterized by the concentration of total suspended solids
210 (TSS) as dry cell weight (DCW), volatile suspended solids (VSS) and soluble chemical
211 oxygen demand (SCOD), following Standard Methods (APHA, 1999). Microalgae were
212 identified by optical microscopy examination (Axioskop 40 Zeiss, Germany), using a photo
213 camera and the Motic Image Plus 2.0 software and conventional taxonomic books (Streble at
214 al., 1987). The initial cells count was 42620000 *Scenedesmus* sp./mL, corresponding to a
215 99.8% of total cells count. Turbidity was determined with a Hanna Microprocessor Turbidity
216 Meter HI93703 and pH with a Crison Portable 506 pH-meter. Turbidity was used to calculate
217 the microalgae harvesting efficiency during magnetic separation.
218
219 ***2.3.4*** *Zeta potential measurements*
220 The zeta potential of the *Scenedesmus* sp. (0.63 g/L) and Fe_3O_4 NPs (0.14 g/L) at pH 7.38
221 were measured using the Zetasizer Nano-ZS (Malvern UK) and calculated according to

Henry's equation at 25°C. Analyses were performed at the *Institut Català de Nanociència i Nanotecnologia* (ICN2), Spain.

2.4 Microalgae harvesting

2.4.1 *Screening of magnetite-based nanoparticles for microalgae harvesting*

The efficiency of microalgae harvesting was evaluated by testing different types of magnetite-based NPs: Fe_3O_4NPs-I, Fe_3O_4NPs-II, Fe_3O_4@SiO-NH_2, Fe_3O_4@CTAB and Fe_3O_4@PEI NPs, in order to compare the effect NPs concentration (I and II NPs type), and the effect of positively coated and non-coated NPs on magnetic microalgae separation. The harvesting efficiency (%) was calculated based on the measurements of turbidity before and after the interaction of microalgae with NPs. Initially, microalgae and NPs were mixed in a weight ratio of 2:1 for 20 min on a shaker at 200 rpm and 25°C (as described in section 2.5.1). Then, magnetic separation was undertaken for another 20 min. Finally, the supernanant turbidity was measured and the harvesting efficiency calculated. All the tests were performed in triplicate. The results were used to determine the best NPs for subsequent process optimization.

2.4.2 *Effect of shaking on microalgae recovery using Fe_3O_4 NPs-I*

The optimization of interactions between NPs and microalgae cells involved studying the effect of shaking before magnetic separation of microalgae. Two types of shaker,orbital and roller, were compared, while non-shaking was used as control. Briefly, 0.2 g/L of Fe_3O_4 NPs-I were added into three vials containing 10 mL of microalgae suspension, two of them were then placed in the orbital and roller shakers, respectively, and the third one was kept without shaking. After 5 min of magnetic separation, the supernatant turbidity was measured and the removal efficiency calculated. All the experiments were performed

247 in triplicate. The effect of shaking was statistically evaluated using the one way analysis of
248 variance (ANOVA).
249
250 ***2.4.3*** *Optimization of the microalgae harvesting efficiency using the response surface*
251 *methodology*
252 Optimum conditions for the removal of microalgae by Fe_3O_4 NPs-I were determined by
253 means of central composite design (CCD) under response surface methodology (RSM)
254 using a combination of mathematical and statistical techniques to evaluate the relative
255 significant factors for the harvesting efficiency. In this study, two three-level full factorial
256 design (3^k), were used. Both of them contained all the possible combinations of factors;
257 contact time, magnetic separation time and concentration of Fe_3O_4 NPs-I, and their levels.
258 The experimental design was set-up based on a central level (0) in the middle point
259 between the lowest (-1) and the highest levels (+1) expressed as normalized values.
260 Therefore, twenty nine experiments were performed for the experimental design with three
261 factors: concentration of Fe_3O_4 NPs-I (0.02, 0.04 and 0.2 g/L), contact time between
262 microalgae and NPs (1, 20 and 60 min) and magnetic separation time (1, 5 and 20 min).
263 The results of the harvesting system were fit to a quadratic model and the quality of the
264 fitted model was quantitatively assessed by the ANOVA to characterize the interaction
265 between independent factors and the microalgae harvesting efficiency. The results were
266 then refined by the Design Expert v6.0 software to fit a quadratic model, with a general
267 expression as shown in Eq. 1:
268
269 $$Y = \beta_0 + \sum_{i=1}^{k} \beta_i X_i + \sum_{i=1}^{k} \beta_{ii} X_i^2 + \sum_{i=1}^{k-1} \sum_{j=2}^{k} \beta_{ij} X_i X_j \qquad (1)$$
270

Where Y is the response (harvesting efficiency), x_i, x_j, …., x_k are input factors (NPs concentration, contact time and separation time), β_0 is the intercept term, β_i (i=1, 2, …, k) is the linear effect, β_{ii} (i=1, 2, …, k) is the squared effect, and β_{ij}(i=1, 2, …, k, j= 1, 2, …, k) is the interaction effect.

The validity of the equation to fit the second order model was verified by the correlation coefficient R^2.

2.4.4 *Adsorption isotherms*

Adsorption isotherm experiments were carried out in a range of concentrations from 0.1 to 1.25 g/L of *Scenedesmus* sp. by dilution with water or concentration via centrifugation. Fe_3O_4 NPs-I were used at the optimal dose previously obtained and pH 7.38 (pH of wastewater). Different isotherm models, Langmuir, Freundlich, and Dubinin–Radushkevich were used for fitting experimental data. They can be expressed in a nonlinear form as shown in eqs. 2-6.

Langmuir isotherm: $$Q_e = \frac{Q_m K_L C_e}{(1+K_L C_e)} \quad (2)$$

Freundlich isotherm: $$Q_e = K_F C_e \, {}^{1}/_{n} \quad (3)$$

Dubinin–Radushkevich isotherm: $$Q_e = Q_m exp^{(-K_{DR}\varepsilon^2)} \quad (4)$$

$$\varepsilon = RTLn[1 + {}^{1}/_{C_e}] \quad (5)$$

$$E = \frac{1}{\sqrt{2K_{DR}}} \quad (6)$$

Where Q_e (g_{DCW}/g_{NPs}) and *Ce* (g/L) are the adsorption capacity and the concentration under equilibrium, respectively, Q_m (g_{DCW}/g_{NPs}) is the maximum adsorption capacity and K_L (L/g)

295 is the Langmuir constant. K_F and 1/n are the Freundlich constants related to the adsorption
296 capacity and intensity, respectively. K_{DR} (mol^2/kJ^2) is Dubinin-Radushkevich isotherm
297 constant, R is the gas constant (8.31 J/molK), T is absolute temperature (K), and E is the
298 apparent energy of adsorption per molecule of adsorbate (kJ/mol) (Babaeivelni et al.,
299 2013).
300
301 ***2.4.5*** *Reusability of magnetite-based nanoparticles*
302 Harvesting costs could be reduced by NPs recovery, which involves firstly the separation
303 of NPs from microalgae and following the regeneration of Fe_3O_4 NPs-I. The regeneration
304 of NPs was accomplished with a slight change of the reported method (Wang et al., 2016).
305 Typically, the NPs and microalgae cells obtained after magnetic separation were suspended
306 in 5 mL of NaOH (0.5 M), by shaking at 200 rpm for 10 min. Then, the suspension was
307 ultrasonicated for 10 min. Following the addition of 2 mL of methanol and 2 mL of
308 chloroform, the resulting solution was ultrasonicated for another 15 min. Finally, Fe_3O_4
309 NPs-I were gathered by using a permanent magnet and washed twice using ultra-pure
310 water. Then, regenerated NPs were tested five times, by repeating the same process, to
311 evaluate the harvesting efficiency after each cycle under the same conditions of microalgae
312 and NPs concentrations.
313
314 ***2.5 Comparison of the magnetic separation with flocculation and gravity settling***
315 Comparison of magnetic separation with algae flocculation and gravity settling was carried
316 out in 200 mL beakers with 150 mL of microalgae suspension. Sedimentation and
317 flocculation assays were performed using the Jar Test procedure under the same conditions
318 of mixing rate and timing. For the flocculation assay 2.5 mL of aqueous solution 1% (w/v)
319 of poly(diallyldimethylammonium chloride(DADM)) (Derypol, Barcelona) was used as

flocculant per 100 mL of algae suspension according to the manufacturer's instructions. The optimal contact time found for microalgae harvesting procedure with NPs, 27 min, was the stirring time for sedimentation an flocculation tests, while the beaker containing 0.14 g NPs (optimal concentration) was shaked for 27 min with the orbital shaker. Following the 27 minute stirring or shaking, the algal biomass was allowed to gravity settle in the sedimentation and flocculation tests. Turbidity measurements were then taken at 2, 4, 8 and 12 min.

2.6 Statystical analysis

The Tukey's method based on one factor ANOVA at the 5% confidence level was used for the statistical analysis, which was performed with SPSS 15.0.1 software (SPSS Inc., USA). Statistically significant differences were reported when the probability of the results (p) value is less than 0.05 assuming the null hypothesis.

3. Results and Discussion

3.1. Characterization of magnetite-based nanoparticles

3.1.1. *Iron concentration in synthesized nanoparticles*

In this study, 5 different types of coated and non-coated magnetite-based NPs were synthesized: Fe_3O_4 NPs-I, Fe_3O_4 NPs-II, Fe_3O_4@SiO-NH_2, Fe_3O_4@CTAB and Fe_3O_4@PEI NPs. As a result of the increase of iron salts during the synthesis process, the iron content increased for Fe_3O_4 NPs-I compared to Fe_3O_4 NPs-II (Table 1). When comparing the iron content of the coated NPs, it is noted that 95.64 % of the Fe_3O_4 NPs were successfully coated to CTAB, while 91.74 % of Fe_3O_4 NPs were coated to PEI. This could be attributed to the high affinity to Fe_3O_4 NPs of the cationic surfactant as compared to the cationic polymer.

345 *3.1.2. TEM-Electron diffraction analysis of synthesized nanoparticles*

346 TEM images and electron diffraction patterns of synthesized NPs are shown in Figure 1.
347 The average size of NPs, listed in Table 1, agrees with literature results for self-made
348 Fe_3O_4 NPs (Fraga-Garcia et al., 2018). The reduction in size compared to commercial
349 Fe_3O_4 NPs (50-100 nm) entails an increase of the specific surface which favors NPs-
350 microalgae interaction resulting in a better harvesting efficiency. Reported studies with
351 *Chlorella vulgaris* reveal a harvesting efficiency of 90% using commercial Fe_3O_4 NPs with
352 concentrations of 10 g/L, hence a minor harvesting efficiency with higher NPs
353 concentrations than our work (Zhu et al., 2017).

354 As shown in Figures 1a-g, a decrease of the aggregation and increase of the dispersion of
355 Fe_3O_4–based NPs was produced by using both the surfactant and the polymer. Besides, all
356 Fe_3O_4–based NPs for the uncoated NPs or the modified ones had the magnetite crystalline
357 structure, as shown in the electron diffraction patterns (Figures 1h-l), which means that the
358 modification of the surface did not affect the crystallinity of Fe_3O_4–based NPs. These
359 results are in agreement with literature (Yazid et al., 2017).

360

361 ***3.2 Optimizing microalgae harvesting efficiency***

362 *3.2.1 Characterization of microalgae and nanoparticles interaction using TEM and SEM*

363 The interaction between microalgae and NPs was checked by characterizing *Scenedesmus*
364 sp. microalgae before and after mixing with NPs using TEM and SEM. The size and
365 morphology of NPs after contact with *Scenedesmus* sp. are illustrated in Figures 2 and 3.
366 The average NPs sizes obtained from TEM images are listed in Table 1. Obviously, the
367 interaction of microalgae with NPs was shown by the increase in the NPs size. Conversely,
368 the crystalline structure of Fe_3O_4–based NPs (Figure 2) was not affected by the interaction
369 with microalgae cells, which is a crucial aspect in the viability of reusing Fe_3O_4–based

NPs. Notice that the crystalline structure of Fe_3O_4@CTAB could not be observed due to an insufficient scattering of electrons from these NPs.

The interaction between microalgae and NPs was further confirmed by SEM. As shown in Figures 3b-f, there was a coverage layer of NPs over the surface of *Scenedesmus* sp. cells.

3.2.2 Screening of magnetite-based nanoparticles for the recovery of microalgae

The screening of Fe_3O_4-based NPs in terms of *Scenedesmus* sp. harvesting efficiency is shown in Figure 4. The experimental conditions are mentioned in section 2.4.1. As can be seen, the highest harvesting efficiency (%) was achieved by Fe_3O_4@SiO-NH_2 (>82%) followed by Fe_3O_4@PEI > Fe_3O_4@CTAB > Fe_3O_4 (I) > Fe_3O_4 (II). Indeed, the highest harvesting efficiencies were obtained with functionalized Fe_3O_4–based NPs, due to the positive functional groups, which enhance the interactions between NPs and microalgae cells (Ge et al, 2015b). However, multi-comparison analyses using the Tukey test only showed significant differences when comparing Fe_3O_4 NPs-I versus Fe_3O_4 NPs-II (p-value <0.05), while no significant differences were observed when comparing Fe_3O_4 NPs-I versus Fe_3O_4@SiO-NH_2, Fe_3O_4@PEI, and Fe_3O_4@CTAB NPs. In consequence, as coated nanoparticles did not show better harvesting efficiency compared to uncoated nanoparticles, the latter were chosen for the optimization experiments. Fe_3O_4 NPs-I nanoparticles were selected due to their lower reagents consumption.

To further illustrate the benefits of adding Fe_3O_4 NPs-I, Figure 5 shows the magnetic separation of microalgae with and without NPs, the former clearly reducing the turbidity of the culture.

3.2.3 Effect of shaking on microalgae recovery using Fe_3O_4 NPs-I

In an attempt to enhance the microalgae harvesting efficiency using Fe_3O_4 NPs-I, the effect of shaking during the contact time between NPs and microalgae before magnetic separation was evaluated. The average values of microalgae harvesting efficiency were found to be 82, 80.7 and 75.5 % by using an orbital shaker, a roller and no agitation, respectively, and with experimental conditions mentioned in section 2.4.1. When applying the Tukey test for all pairwise multiple comparison procedures, the only statistically significant differences were found by using orbital or roller shakers versus no shaking, while no statistical difference was found between orbital and roller shakers. Therefore, agitation itself was the important factor for the improvement of the harvesting efficiency. Since the orbital shaker showed slightly better biomass recovery results, the following experiments were performed with this shaking device.

3.2.4 Central composite design with a response surface method to optimize the harvesting efficiency using Fe_3O_4 NPs-I

Optimization and modelling of the microalgae harvesting efficiency were performed by using the central composite design (CCD) under the response surface methodology (RSM). The range and level of experimental variables used in this studyare shown in Table 2.

From the experimental design a second order equation (7), was obtained after studying the three independent factors. The R^2 value of this model was 0.87.

Harvesting efficiency % = 63.45 +1.19(Contact time) +0.63(Separation time) +71.91(NPs concentration) -0.011(Contact time)(Separationtime) -1.19(Contact time)(NPs concentration) -0.0114(Contact time)^2 (7)

418 The fitness and validity of the model were evaluated by the ANOVA for the combined
419 experimental design used. According to the statistical model, all the terms were significant
420 ($p<0.05$) and the Lack of fit F value (0.44) implies that the Lack of fit was not significant
421 ($p>0.05$), hence the quadratic model was valid for the prediction of experimental data. Thus,
422 all the terms of equation (7) are statistically significant (Subbalaxmi et al., 2016).
423 The highest linear coefficient value of NPs concentration implies its significant effect on the
424 microalgae harvesting efficiency, which means that the microalgae harvesting efficiency is
425 enhanced by increasing the concentration of NPs, which agrees with literature (Seo et al.
426 2015). In addition, the negative value of the quadratic coefficient indicates the existence of
427 optimum values for the microalgae harvesting efficiency.
428 According to this model (equation 7), the maximum harvesting efficiency was obtained by
429 solving the regression model at 0.14 g/L of Fe_3O_4 NPs-I, 27 min of contact time between
430 microalgae and NPs and 8 min of magnetic separation time, leading to a theoretical
431 microalgae recovery of 95.68 %.
432 These results are similar to those reported by Hu et al. (2013) using the marine microalgae
433 *Nannochloropsis maritima*. They also reached removals of 95%, but after 4 min of magnetic
434 separation (8 min in this study) and with a concentration of 0.12 g/L of Fe_3O_4 NPs (0.14 g/L
435 in this study). Other studies obtain similar harvesting efficiencies with lower concentrations,
436 for instance Hu et al. (2014) report a 97% harvesting efficiency with 0.02 g/L for *Chlorella*
437 *ellipsoidea*, but the nanoparticles are coated with PEI, which enhances microalgae-NP
438 interaction. Also, Wang et al. (2014) report a harvesting efficiency of 95% using 0.025 g/L of
439 NPs for *Botryococcus braunii* and 0.12 g/L for *Chlorella ellipsoidea*, also with Fe_3O_4 NPs
440 coated with cationic polyacrylamide (CPAM). This latter difference in NPs concentration to
441 obtain the same harvesting efficiency for two different microalgae species evidences the
442 difficulty to compare magnetic harvesting processes.

Figure 6 shows the response surface (according to equation 7) of microalgae harvesting efficiency as a function of the Fe_3O_4-based NPs concentration and the magnetic separation time, at three different contact times. From the comparison it can be concluded that with low contact times of 1 min (Figure 6a) the harvesting efficiency increases along with the magnetic separation time and Fe_3O_4–based NPs concentration. However, after 20 min of contact (Figure 6b) the increase of harvesting efficiency along with the magnetic separation time and Fe_3O_4–based NPs concentration is not so remarkable, although better microalgae recoveries are obtained. Finally, after 60 min of contact (Figure 6c) the magnetic separation time and Fe_3O_4-based NPs concentration do not have any significant impact on the harvesting efficiency.

On one hand, this could be due to the fact that at low contact times, the magnetic separation time also acts as a contact time between microalgae and NPs. However, as contact time increases, the improvement in the harvesting efficiency is less dependent on the NPs concentration and magnetic separation time. This could be attributed to the fact that with high contact times, even at the lowest NPs concentration, the NPs dispersion is good enough to allow the interaction between microalgae and NPs still reporting good harvesting efficiency. This is in agreement with the optimum contact time of 27 min. Therefore, NPs-microalgae contact time, previous or during the magnetic separation, is a key parameter for improving the harvesting efficiency.

3.3 Adsorption isotherms and possible mechanisms of interaction

The equilibrium relationship between the amount of *Scenedesmus* sp. per gram of Fe_3O_4–based NPs was determined by the adsorption isotherms in order to evaluate the affinity of NPs for microalgae. In this study, Langmuir, Freundlich, and Dubinin–Radushkevich isotherm models were used due to their relative simplicity and reasonable accuracy

(Nassar, 2010). The Langmuir model assumes that microalgae harvesting occurs on a homogenous surface by monolayer, while the Freundlich model assumes that it occurs on a heterogenous surface of the NPs. The Dubinin-Radushkevich isotherm model was used to estimate the possible mechanism of interaction as physisorption or chemisorption process. Model fitting of experimental data using Langmuir and Freundlich isotherms are shown in Figure 7. Estimated parameters for all models were calculated using non-linear regressions, and their values with the corresponding correlation coefficients (R^2) are presented in Table 6. The Langmuir model showed the highest R^2 value (0.99) in comparison with the other ones, suggesting that microalgae harvesting could work as a monolayer coverage on Fe_3O_4 NPs-I. Thus, the maximum monolayer adsorption capacity (Q_m) obtained was 3.49 mg/gFe_3O_4 NPs-I. Moreover, the high value of K_L indicates that *Scenedesmus* sp. microalgae cells were bonded strongly by Fe_3O_4 NPs (Xu et al. 2011). The type of isotherm was found to be highly favorable due to the low separation factor constant (R_L=0.36), which is in the range between 0 and 1 (Hasanzadeh et al. 2017). In addition, for the Freundlich isotherm model, Fe_3O_4 NPs-I enhanced the recovery of *Scenedesmus* sp. since the 1/n value was 0.51, which is in the range between 0 and 1 (Chaudhry et al., 2017).

As indicated in Table 3, the calculated parameter of the apparent energy (E) of the Dubinin–Radushkevich isotherm was 8.73 kJ/mol. Therefore, harvesting of *Scenedesmus* sp. microalgae by Fe_3O_4 NPs-I could be attributed to chemisorption because the magnitude of E was higher than 8.00 kJ/mol (Chaudhry et al., 2017).

It is well known that the agglomeration phenomena occurs when nanoparticles are dispersed in liquid media (Figure 1). This problem can be partially corrected using self synthesized nanoparticles with proper stabilizers. However, agglomeration cannot be completely avoided and, consequently, some active sites of the adsorbent will not be

493 available. Thus, it is clear that the use of any isotherm as an interaction between an ideal
494 solid surface and an adsorbate is a simplification. It is also applicable to the harvesting
495 yields, which would be better if no agglomeration occurred. This must be taken into
496 account when interpreting these results.
497 Further investigation of the possible mechanism of interaction between the Fe_3O_4–based
498 NPs and microalgae was performed by measuring their zeta potential at pH 7.38 (the pH of
499 the culture). The zeta potential value of the microalgae suspension was -3.7 mV, while the
500 value for the Fe_3O_4 NPs-I was +3.9 mV. Hence, a strong electrostatic attraction was
501 observed between *Scenedesmus* sp. and Fe_3O_4 NPs-I. This possible mechanism of
502 interaction was in agreement with the findings of Xu et al. (2011), who used Fe_3O_4 NPs for
503 harvesting *Botryococcus Braunii* and *Chlorella Ellipsoidea* cells. To our knowledge, this
504 had not been reported for *Scenedesmus* sp.
505
506 ***3.4 Regeneration and reusability of Fe_3O_4 NPs***
507 The feasibility of microalgae harvesting using NPs but also the downstream processing of
508 harvested biomass to obtain biofuels or bioproducts, call for NPs recovery and
509 regeneration. In spite of this, such issues have been hardly addressed. According to Wang
510 et al., (2016), the combination of strong alkaline treatments and ultrasonication detachment
511 showed the highest detachment potential of magnetite NPs if compared to the application
512 of alkaline or ultrasonication methods separatedly. As a result of the application of the
513 modified method, Fe_3O_4 NPs-I could successfully be re-used 5 times for harvesting the
514 microalgae *Scenedesmus* sp., with only a slight decrease in the harvesting efficiency from
515 90 to 84.1% (Figure 8). The break-up of Fe_3O_4 NPs-I from microalgae at high pH values
516 could be a result of a weaker electrostatic attraction between microalgae and NPs, due to
517 an increased negative charge of NPs and microalgae cells in a strong alkaline medium (Seo
518 et al., 2014). Besides, the use of a methanol and chloroform mixture combined with the

519 ultrasonic treatment could have enhanced the separation between microalgae cells and NPs
520 (Lin et al., 2015). In any case, the combination of strong alkaline medium and
521 ultrasonication treatments used in this study implies the lysis of microalgae. However, this
522 could have some beneficial effects for some very extended applications of residual
523 microalgae such as the extraction of lipids from microalgae cells or anaerobic digestion,
524 which would be useful for the subsequent valorization of the harvested microalgae (e.g.
525 obtention of biogas or biodiesel) (Choy et al., 2014; Ramos-Suárez et al., 2014). If the
526 objective is to recover living microalgae, it is evident that this procedure should be
527 modified.
528 This study showed how the modified combined method only led to a small decrease in the
529 harvesting efficiency after 5 cycles (5.9 %), improving the original regeneration method,
530 which resulted in a decrease of 22.2 % (Wang et al., 2016). This could be attributed to the
531 use of a lower concentration of NaOH in the detachment process and a longer
532 ultrasonication time. Therefore, the proposed modified regeneration method, by using a
533 combination of strong alkaline medium with a lower alkaline concentration and prolonged
534 sonication time, enhances the potential efficiency of NPs as compared to previously used
535 methods (Wang et al., 2016; Lin et al., 2015; Prochazkova et al., 2013b).
536 Moreover, it can be hypothesized that the loss of nanoparticles after each cycle is not
537 significant, given the low decrease in the harvesting efficiencies when using the same
538 sample without adding fresh nanoparticles, although a rigorous iron mass balance was not
539 conducted.

3.5 Comparison of magnetic separation with flocculation and sedimentation

The proposed magnetic separation method was finally compared with gravity settling and flocculation-sedimentation, which are among the most commonly used processes for microalgae recovery.

Figure 9 shows the harvesting efficiency over time for gravity settling, flocculation-sedimentation and magnetic separation. Gravity settling clearly showed the worst results in terms of harvesting efficiency (67%). Note that this final efficiency is similar to the independent term in equation 7, indicating that indeed it could be attributed to sedimentation.

Conversely, flocculation-sedimentation showed a harvesting efficiency more similar to magnetic separation (around 90%). However, at short times, flocculation performed better. Additionally, some authors point out that the presence of other microorganisms can improve sedimentation as a consequence of bioflocculation phenomenon (Nguyen et al., 2019). As discussed previously, contact time increases the harvesting efficiency of magnetic separation. Nevertheless, after only 8 minutes (the optimum separation time according to equation 7), magnetic separation performed slightly better than flocculation. Taking into account that nanoparticles can be regenerated while flocculants cannot, magnetic separation appears as a potential sustainable alternative for microalgae harvesting.

4 Conclusions

In this study, the harvesting efficiency of the microalgae *Scenedesmus sp*. was evaluated by using different Fe_3O_4-based nanoparticles as adsorbents. Naked, coated and functionalized Fe_3O_4-based nanoparticles were used. All the synthesized magnetite-based NPs showed a high potential efficiency for microalgae harvesting, but the naked nanoparticles (Fe_3O_4 NPs-I) performed better. Response surface methodology indicated that the optimum

harvesting conditions were 0.14 g/L of naked Fe_3O_4 NPs-I, 27 min of contact time and 8 min of magnetic separation time. Monolayer adsorption was found to be the main mechanism for microalgae recovery due to the high correlation coefficient of the Langmuir isotherm model, yielding a maximum adsorption capacity, 3.49 g_{DCW}/g_{NPs} for *Scenedesmus* sp. using Fe_3O_4NPs-I. The electrostatic interaction mechanism is proposed to describe the interaction between microalgae cells and NPs. Reactivation of Fe_3O_4NPs-I was successfully achieved using a low concentration of alkali combined with ultrasonication, which allowed for NPs recycling during at least 5 cycles. Magnetic separation clearly outperformed gravity sedimentation, and only slightly flocculation, considering that this latter process was performed according to the manufacturer's instructions.

Further research should be focused on more general aspects to evaluate this technology in terms of cost analysis, energy consumption and environmental impact assessment.

Acknowledgements

Authors wish to thank the finantial support of Xarxa de Referencia de Biotecnologia and the Spanish Ministry of Economy and Competitiveness (FOTOBIOGAS project CTQ2014-57293-C3-3R). The author Ahmad Abo Markeb appreciated and would like to thank the Ministry of Higher Education of Egypt for the PhD external mission grant. The authors are grateful to Dulce Maria Arias and Estel Rueda from the Universitat Politècnica de Catalunya-BarcelonaTech, Gerardo González from the Universidad Politécnica del Estado de Morelos (México) and Andrés Rincón from the Universidad de Santander (Colombia) for their contribution to the microalgae culture. The contribution of Humbert Salvadó from the University of Barcelona in the microalgae identification is appreciated. The authors would like to thank Amirali Yazdi, at *Institut Català de Nanociència i Nanotecnologia* (ICN2), Spain, for his help to measure the zeta potential values.

591

592 **References**

593 Abo Markeb, A., Alonso, A., Dorado, A.D., Sánchez, A., Font, X. 2016. Phosphate removal
594 and recovery from water using nanocomposite of immobilized magnetite
595 nanoparticles on cationic polymer. Environ. Technol. 37(16), 2099-2112.

596 APHA, AWWA and WPCF, 1999. Standard Methods for examination of water and
597 wastewater, American Public Health Association, Washington.

598 Arbib, Z., Ruiz, J., Álvarez Díaz, P., Garrido-Pérez, C., Perales, J.A., 2014. Capability of
599 different microalgae species for phytoremediation processes: Wastewater tertiary
600 treatment, CO_2 bio-fixation and low cost biofuels production. Water Res. 49,465-474.

601 Arias, D.M., Solé-Bundó, M., Garfí, M., Ferrer, I.,García, J., Uggetti, E., 2018. Integrating
602 microalgae tertiary treatment into activated sludge systems for energy and resource
603 recovery. Bioresource Technol. 247, 513-519.

604 Asfaram, A., Ghaedi, M., Yousefi, F., Dastkhoon, M., 2016. Experimental design and
605 modeling of ultrasound assisted simultaneous adsorption of cationic dyes onto ZnS:
606 Mn-NPs-AC from binary mixture. Ultrason. Sonochem. 33, 77-89.

607 Babaeivelni, K., Khodadoust, A.P., 2013. Adsorption of fluoride onto crystalline titanium
608 dioxide: Effect of pH, ionic strength, and co-existing ions. J. Colloid Interface Sci.
609 394, 419-427.

610 Chaudhry, S.A., Zaidi, Z., Siddiqui, S.I., 2017. Isotherm, kinetic and thermodynamics of
611 arsenic adsorption onto Iron-Zirconium Binary Oxide-Coated Sand (IZBOCS):
612 Modelling and process optimization. J. Mol. Liq. 229, 230-240.

613 Choy, W.-Y., Kim G.V., Lee S.-Y.and Lee H.-Y., 2014. Biodiesel Production from
614 *Scenedesmus* sp. through Optimized in situ Acidic Transesterification Process. Chem.
615 Biochem. Eng. Q., 28 (3), 367-374.

616 Dassey, A.J., Theegala, C.S., 2013. Harvesting economics and strategies using centrifugation
617 for cost effective separation of microalgae cells for biodiesel applications.
618 Bioresource Technol., 128, 241-245.

619 Fraga-García, P., Kubbutat, P., Brammen, M., Schwaminger, S. and Berensmeier, S., 2018.
620 Bare Iron Oxide Nanoparticles for Magnetic Harvesting of Microalgae: From
621 Interaction Behavior to Process Realization. Nanomaterials, 8, 292.

622 Ge, S., Agbakpe, M., Wu, Z., Kuang, L., Zhang, W., Wang, X., 2015a. Influences of Surface
623 Coating, UV Irradiation and Magnetic Field on the Algae Removal Using Magnetite
624 Nanoparticles. Environ. Sci. Technol. 49(2), 1190-1196.
625 Ge, S., Agbakpe, M., Wu, Z., Zhang, W., Kuang, L., 2015b. Heteroaggregation between PEI-
626 Coated Magnetic Nanoparticles and Algae: Effect of Particle Size on Algal
627 Harvesting Efficiency. ACS Appl. Mater. Interfaces 7, 6102-6108.

628 Gutiérrez, R., Ferrer, I., González-Molina, A., Salvadó, H., García, J., Uggetti, E., 2016.
629 Microalgae recycling improves biomass recovery from wastewater treatment high rate
630 algal ponds. Water Res. 106, 539-549.
631 Gutiérrez, R., Ferrer, I., García, J., Uggetti, E., 2015a. Influence of starch on microalgal
632 biomass recovery, settleability and biogas production. Bioresource Technol. 185, 341-
633 345.
634 Gutiérrez, R., Passos, F., Ferrer, I., Uggetti, E., García, J., 2015b. Harvesting microalgae
635 from wastewater treatment systems with natural flocculants: Effect on biomass
636 settling and biogas production. Algal Res. 9, 204-211.
637 Hasanzadeh, R., Moghadam, P.N., Bahri-Laleh, N., Sillanpää, M. , 2017. Effective removal
638 of toxic metal ions from aqueous solutions: 2-Bifunctional magnetic nanocomposite

base on novel reactive PGMA-MAn copolymer@Fe_3O_4 nanoparticles. J. Colloid Interface Sci. 490, 727-746.

Hu, Y.-R., Wang, F., Wang, S.-K., Liu, C.-Z., Guo, C., 2013. Efficient harvesting of marine microalgae *Nannochloropsis maritima* using magnetic nanoparticles. Bioresource Technol. 138, 387-390.

Jha, D., Jain, V., Sharma, B., Kant, A., Garlapati, V.K., 2017. Microalgae-based Pharmaceuticals and Nutraceuticals: An Emerging Field with Immense Market Potential. Chem. Bio. Eng. Rev. 4(4), 257-272.

Khan, M.I., Shin, J.H., Kim, J.D., 2018. The promising future of microalgae: current status, challenges, and optimization of a sustainable and renewable industry for biofuels, feed, and other products. Microb. Cell Fact. 17, 36.

Khoshnevisan, K., Barkhi, M., Zare, D., Davoodi, D., Tabatabaei, M., 2012. Preparation and Characterization of CTAB-Coated Fe_3O_4 Nanoparticles. Synth. React. Inorg. M. 42(5), 644-648.

Kumar Gupta, V., Agarwal, S., Asif, M., Fakhri, A., Sadeghi, N., 2017. Application of response surface methodology to optimize the adsorption performance of a magnetic graphene oxide nanocomposite adsorbent for removal of methadone from the environment. J. Colloid Interface Sci. 497, 193-200.

Lin, Z., Xu, Y., Zhen, Z., Fu, Y., Liu, Y., Li, W., Luo, C., Ding, A., Zhang, D., 2015. Application and reactivation of magnetic nanoparticles in *Microcystis aeruginosa* harvesting. Bioresource Technol. 190, 82-88.

Milano, J., Ong, H.C., Masjuki, H.H., Chong, W.T., Lam, M.K., Loh, P.K., Vellayan, V., 2016. Microalgae biofuels as an alternative to fossil fuel for power generation. Renew. Sust. Energ. Rev. 58, 180-197.

663 Nassar, N.N., 2010. Rapid removal and recovery of Pb(II) from wastewater by magnetic
664 nanoadsorbents. J. Hazard. Mater. 184 (1–3), 538-546.
665 Nguyen, T.D.P, Le, T.V.A., Show, P.L., Nguyen, T.T., Tran, M.H., Tran, T.N.T, Lee, S.Y.,
666 2019. Bioflocculation formation of microalgae-bacteria in enhancing microalgae
667 harvesting and nutrient removal from wastewater effluent. Bioresource Technol. 272,
668 34-39.
669 Özçimen, D., İnan, B., Morkoç, O., Efe, A., 2017. A Review on Algal Biopolymers. J. Chem.
670 Eng. Res. Updat. 4, 7-14.
671 Passos, F., Gutiérrez, R., Brockmann, D., Steyer, J.-P., García, J., Ferrer, I., 2015. Microalgae
672 production in wastewater treatment systems, anaerobic digestion and modelling using
673 ADM1. Algal Res. 10, 55-63.
674 Procházková, G., Šafařík, I., Brányik, T. (2012) Surface Modification of *Chlorella Vulgaris*
675 Cells Using Magnetite Particles. Procedia Eng. 42, 1778-1787.
676 Prochazkova, G., Safarik, I. and Branyik, T., 2013a. Harvesting microalgae with microwave
677 synthesized magnetic microparticles. Bioresource Technol. 130, 472-477.
678 Prochazkova, G., Podolova, N., Safarik, I., Zachleder, V. and Branyik, T., 2013b.
679 Physicochemical approach to freshwater microalgae harvesting with magnetic
680 particles. Colloids Surf. B: Biointerfaces 112, 213-218.
681 Ramos-Suárez, J.L., Martínez, A., Carreras, N., 2014. Optimization of the digestion process
682 of *Scenedesmus* sp. and *Opuntia maxima* for biogas production. Energ. Convers.
683 Manage. 88, 1263-1270.
684 Schwertmann, U., Cornell, R.M., 2007. Iron Oxides in the Laboratory, pp. 135-140, Wiley-
685 VCH Verlag GmbH.

686 Seo, J.Y., Lee, K., Lee, S.Y., Jeon, S.G., Na, J.-G., Oh, Y.-K., Park, S.B., 2014. Effect of
687 barium ferrite particle size on detachment efficiency in magnetophoretic harvesting of
688 oleaginous *Chlorella* sp. Bioresource Technol. 152, 562-566.
689 Seo JY, Lee K, Praveenkumar R, Kim, B., Lee, S.Y., Oh, Y.K., Park, S.B., 2015. Tri-
690 functionality of Fe_3O_4-embedded carbon microparticles in microalgae harvesting.
691 Chem Eng J. 280, 206–214.

692 Singh, N.K., Dhar, D.W., 2011. Microalgae as second generation biofuel. A review.
693 Agronomy Sust. Developm. 31, 605-629.
694 Streble, H., Krauter, D.,1987. Atlas de los microorganismos de agua dulce, La vida en una
695 gota de agua. Omega, Barcelona (Spain).
696 Subbalaxmi, S., Murty, V.R., 2016. Process optimization for tannase production by *Bacillus*
697 *gottheilii* M2S2 on inert polyurethane foam support. Biocatal. Agric. Biotechnol. 7,
698 48-55.
699 Valigore, J.M., Gostomski, P.A., Wareham, D.G., O'Sullivan, A.D., 2012. Effects of
700 hydraulic and solids retention times on productivity and settleability of microbial
701 (microalgal-bacterial) biomass grown on primary treated wastewater as a biofuel
702 feedstock. Water Res. 46, 2957-2964.

703 Vandamme, D., Foubert, I., Muylaert, K., 2013. Flocculation as a low-cost method for
704 harvesting microalgae for bulk biomass production. Trends Biotechnol. 31(4), 233-
705 239.

706 Wang, S.-K., Wang, F., Hu, Y.-R., Stiles, A.R., Guo, C., Liu, C.-Z., 2014. Magnetic
707 Flocculant for High Efficiency Harvesting of Microalgal Cells. ACS Appl. Mater.
708 Interfaces 6(1), 109-115.

709 Wang, T., Yang, W.-L., Hong, Y., Hou, Y.-L., 2016. Magnetic nanoparticles grafted with
710 amino-riched dendrimer as magnetic flocculant for efficient harvesting of oleaginous
711 microalgae. Chem. Eng. J. 297, 304-314.
712 Xu, L., Guo, C., Wang, F., Zheng, S., Liu, C.-Z., 2011. A simple and rapid harvesting method
713 for microalgae by in situ magnetic separation. Bioresource Technol. 102(21), 10047-
714 10051.
715 Yazid, N.A., Barrena, R., Sánchez, A., 2017. The immobilisation of proteases produced by
716 SSF onto functionalized magnetic nanoparticles: Application in the hydrolysis of
717 different protein sources. J. Mol. Catal.B: Enzym.133(1), S230-S242.
718 Zhang, L., He, Y., Goswami, N., Xie, J., Zhang, B., Tao, X., 2016. Uptake and effect of
719 highly fluorescent silver nanoclusters on *Scenedesmus obliquus*. Chemosphere 153,
720 322-331.
721 Zhu, L.D., Hiltunen, E., Li, Z., 2017. Using magnetic materials to harvest microalgal
722 biomass: evaluation of harvesting and detachment efficiency. Environ. Technol. DOI:
723 10.1080/09593330.2017.1415379

Table 1. Iron content and average size before and after contact with microalgae of the five types of synthesized nanoparticles.

Nanoparticles	Iron concentration (mg_{Fe}/g_{NPs})	Average size before microalgae contact (nm)	Average size after microalgae contact (nm)
Fe_3O_4 (I)	579.1 ± 11.3	11.15 ± 1.57	14.58 ± 1.38
Fe_3O_4 (II)	699.0 ± 4.9	11.73 ± 1.61	13.77 ± 3.05
Fe_3O_4@CTAB	668.6 ± 4.6	11.49 ± 1.83	15.08 ± 2.04
Fe_3O_4@PEI	641.3 ± 3.0	12.57 ± 1.86	15.52 ± 2.07
Fe_3O_4@SiO-NH_2	541.7 ± 6.1	13.68 ± 1.77	18.31 ± 3.16

Table 2. Experimental design used for microalgae harvesting efficiency (H.E.) using Fe_3O_4 NPs-I.

Experiment	Contact time (min)	Magnetic separation time (min)	NPs concentration (g/L)	H.E. (%)
1	1	1	0.2	76.43
2	1	1	0.04	61.91
3	1	1	0.02	57.02
4	1	5	0.2	86.12
5	1	5	0.04	68.23
6	1	5	0.02	65.34
7	1	20	0.2	89.29
8	1	20	0.04	84.00
9	1	20	0.02	80.40
10	20	1	0.2	93.24
11	20	1	0.04	87.75
12	20	1	0.02	83.14
13	20	5	0.2	94.37
14	20	5	0.04	92.06
15	20	5	0.04	81.80
16	20	5	0.04	92.48
17	20	5	0.02	83.43
18	20	20	0.2	93.64
19	20	20	0.04	92.39
20	20	20	0.02	92.91
21	60	1	0.2	94.82
22	60	1	0.04	93.83
23	60	1	0.02	94.26
24	60	5	0.2	93.26
25	60	5	0.04	91.87
26	60	5	0.02	92.27
27	60	20	0.2	94.52
28	60	20	0.04	93.48
29	60	20	0.02	93.55

Table 3. Langmuir, Freundlich and Dubinin–Radushkevich isotherm parameters for *Scenedesmus* sp. microalgae adsorption on Fe_3O_4 NPs-I.

Langmuir	**$Q_m(g_{DCW}/g_{NPs})$**	3.49
	K_L (L/mg)	9.06
	R^2	0.99
	R_L	0.36
Freundlich	**K_F ($mg^{1-(1/n)}L^{1/n}g^{-1}$)**	4.86
	1/n	0.51
	R^2	0.98
Dubinin–Radushkevich	**Q_m(g/g)**	2.93
	K_{DR} (mol^2/kJ^2)	1.66E-8
	R^2	0.91
	E (kJ/mol)	8.73

Figure
Click here to download high resolution image

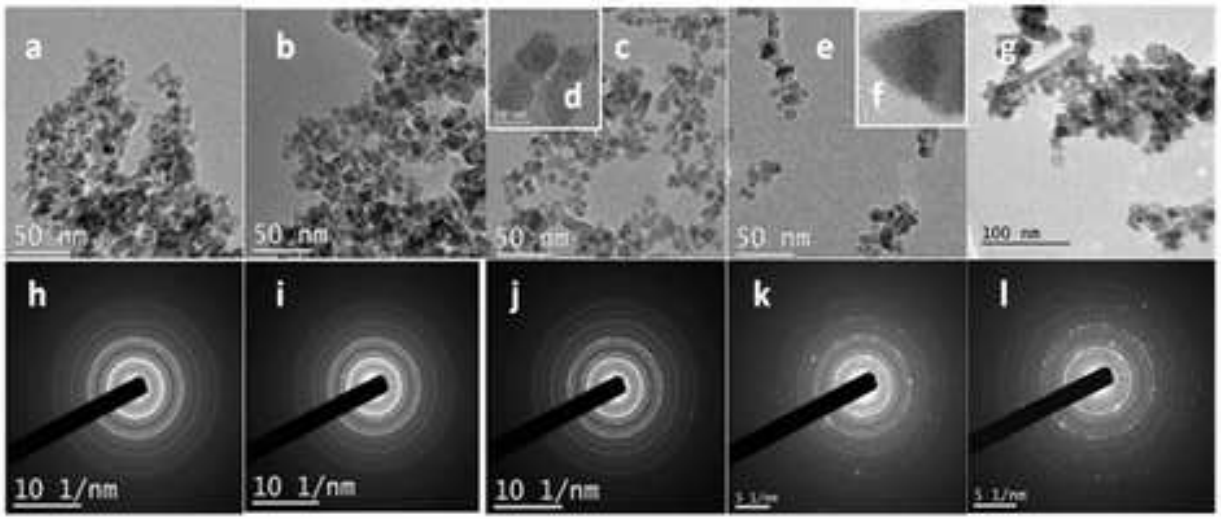

Figure 1. TEM images of: (a) Fe_3O_4 NPs-I; (b) Fe_3O_4 NPs-II; (c,d) Fe_3O_4@CTAB NPs; (e,f) Fe_3O_4@PEI NPs; (g) Fe3O4@SiO-NH_2, and Electron Diffraction patterns of: (h) Fe_3O_4 NPs-I; (i) Fe_3O_4 NPs-II; (j) Fe_3O_4@CTAB NPs; (k) Fe_3O_4@PEI; (l) Fe_3O_4@SiO-NH_2.

Figure
Click here to download high resolution image

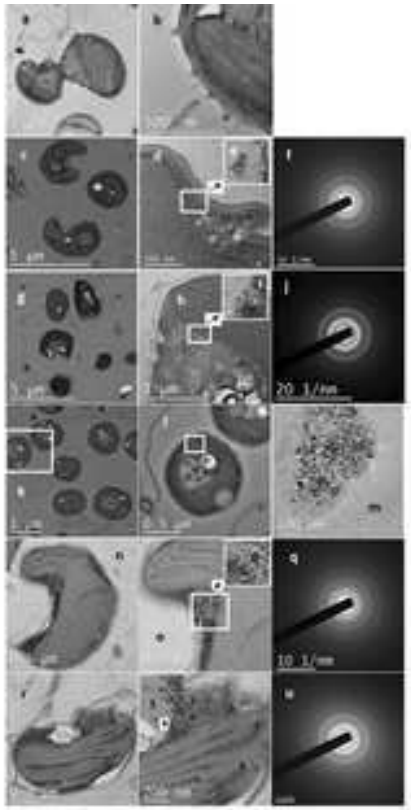

Figure 2. HR-TEM images of: (a, b) *Scenedesmus* sp. microalgae, and *Scenedesmus* sp. with (c, d) Fe_3O_4 NPs-I, (g, h) Fe_3O_4 NPs-II, (k, l) Fe_3O_4@CTAB, (n, o) Fe_3O_4@PEI, (r, s) Fe_3O_4@SiO-NH_2 NPs; (e) Fe_3O_4 NPs-I, (i) Fe_3O_4 NPs-II, (m) Fe_3O_4@CTAB, (p) Fe_3O_4@PEI, (t) Fe_3O_4@SiO-NH_2 inside *Scenedesmus* sp.; and Electron Diffraction pattern of (f, j, q, u) Fe_3O_4 NPs-I, Fe_3O_4NPs-II, Fe_3O_4@PEI and Fe_3O_4@SiO-NH_2 NPs respectively.

Figure
Click here to download high resolution image

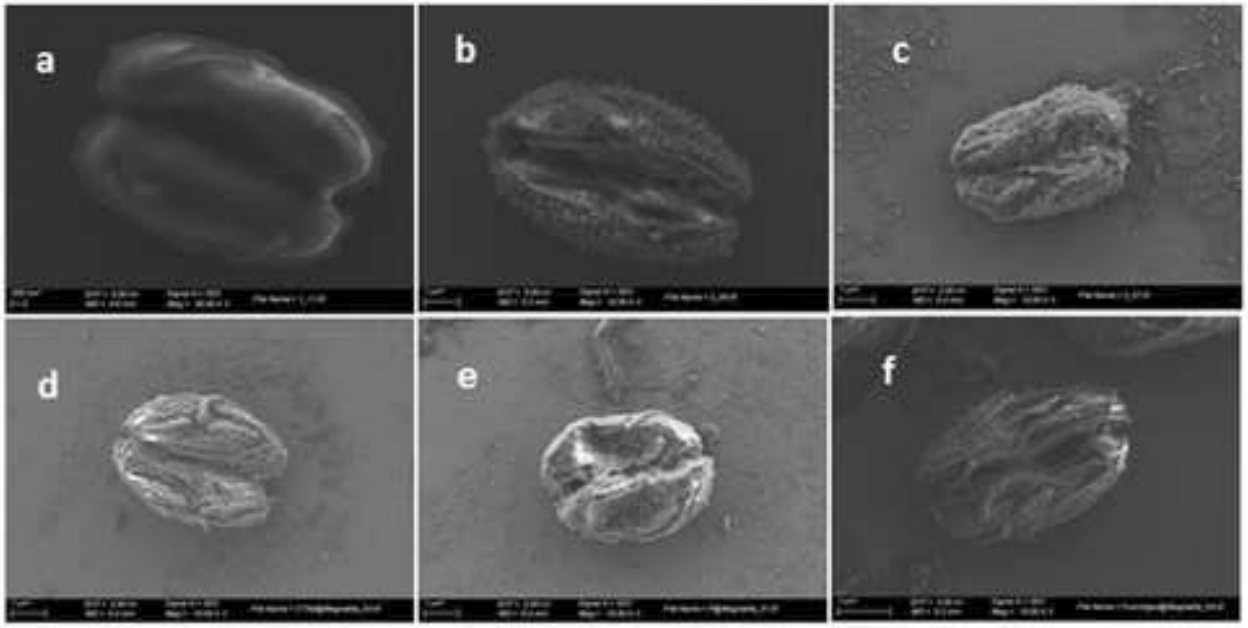

Figure 3. SEM images of: (a) naked *Scenedesmus* sp. microalgae, and *Scenedesmus* sp. after contact with NPs: (b) Fe_3O_4 NPs-I, (c) Fe_3O_4 NPs-II, (d) Fe_3O_4@CTAB, (e) Fe_3O_4@PEI, (f) Fe_3O_4@SiO-NH_2.

Figure
Click here to download high resolution image

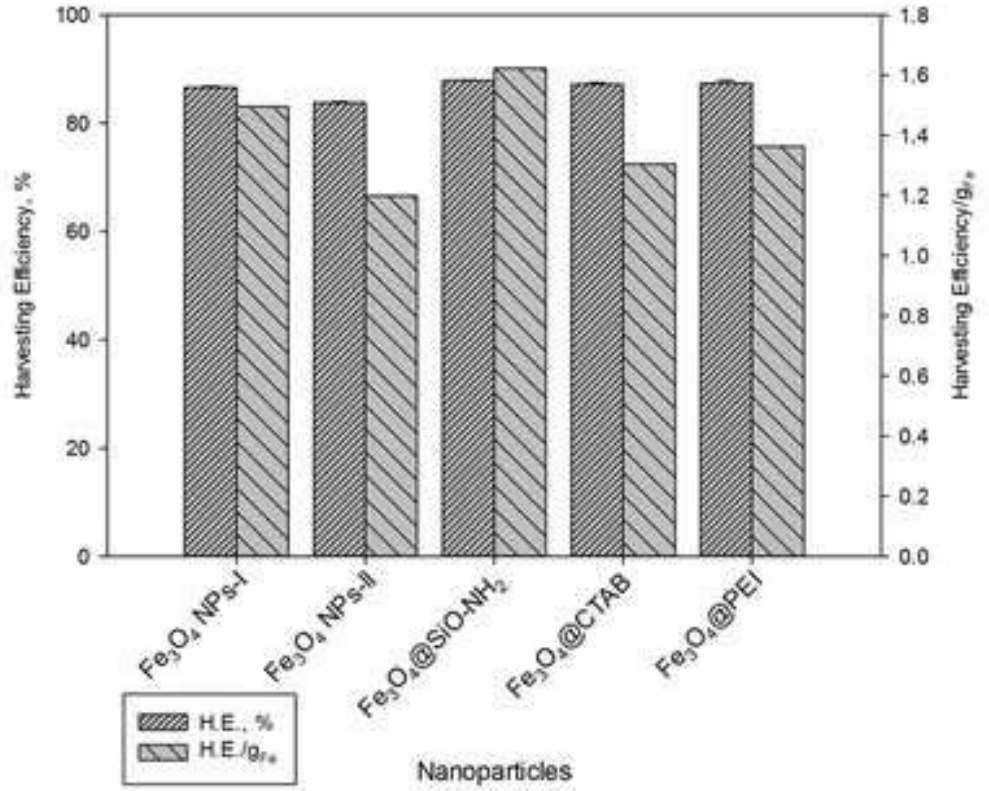

Figure 4. Screening of the harvesting efficiency (H.E.), and H.E./gr_e of *Scenedesmus* sp. using Fe_3O_4 based NPs.

Figure
Click here to download high resolution image

Figure 5. Magnetic separation of microalgae: (A) Without NPs and (B) With Fe_3O_4 NPs-I (0.25 g/L of NPs and 20 min of magnetic separation time).

Figure
Click here to download high resolution image

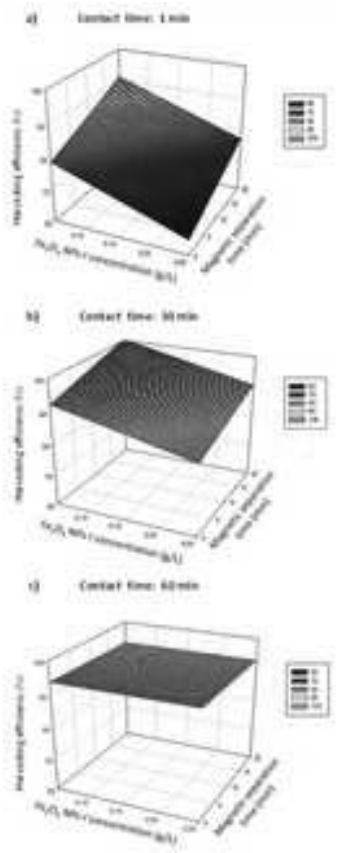

Figure 6. Response surface of microalgae harvesting efficiency as a function of Fe_3O_4 NPs-I concentration and magnetic separation time, in three diferent contact times: a) 1 min, b) 20 min and c) 60 min.

Figure
Click here to download high resolution image

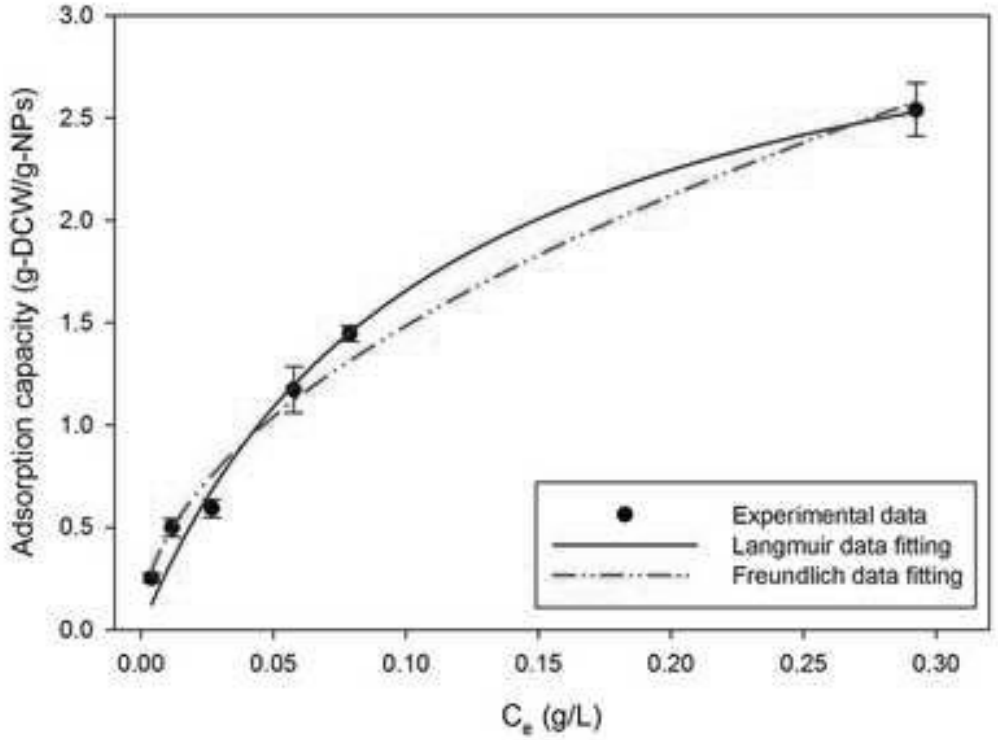

Figure 7. Adsorption isotherm of *Scenedesmus* sp. microalgae using Fe_3O_4 NPs-I.

Figure
Click here to download high resolution image

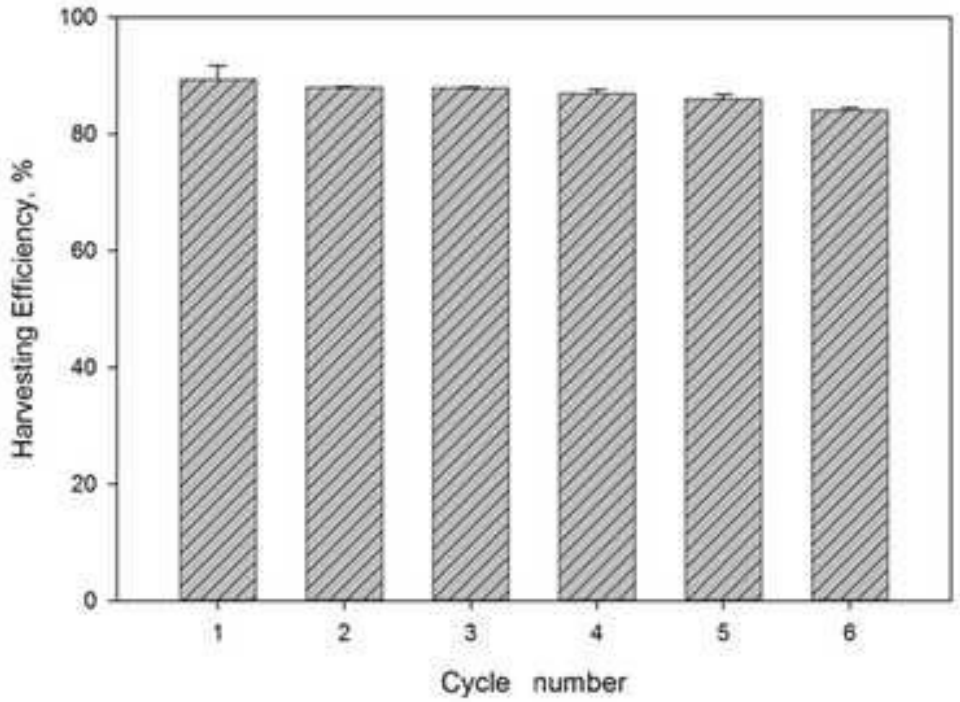

Figure 8. Harvesting efficiency of *Scenedesmus* sp. microalgae using Fe_3O_4 NPs-I.

Figure
Click here to download high resolution image

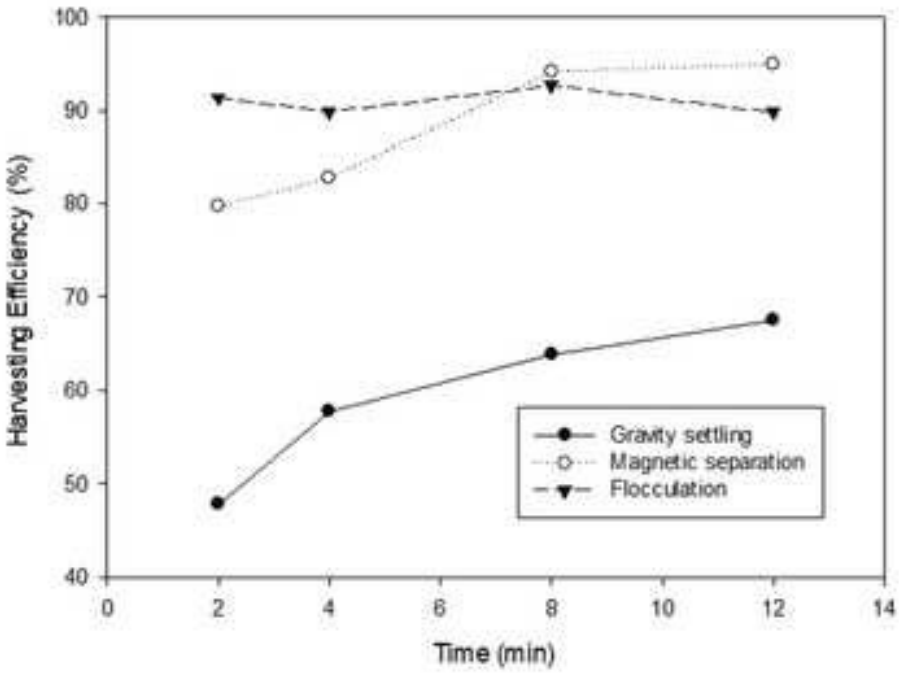

Figure 9. Comparison of the microalgae harvesting efficiency (%) over 12 minutes of separation time for gravity settling, flocculation-sedimentation with poly(diallyldimethylammonium chloride(DADM)) and magnetic separation with NPs.